

**STRAIN-RATE AND TEMPERATURE EFFECTS ON KINETICS OF PHASE TRANSITIONS IN ALBITE.**

**M. Sims**<sup>1</sup>, M. Rucks<sup>1</sup>, S. Lobanov<sup>1</sup>, J. Young<sup>1</sup>, J.A. Daly<sup>1</sup>, A. Pakhomova<sup>2</sup>, Z. Konopkova<sup>2,3</sup>, H.P. Liermann<sup>2</sup>, R. Hrubiak<sup>4</sup>, M.L. Whitaker<sup>1,5</sup>, T.D. Glotch<sup>1</sup>, and L. Ehm<sup>1,5</sup>, <sup>1</sup>Department of Geosciences, Stony Brook University, Stony Brook, NY 11794-2100 (melissa.sims@stonybrook.edu), USA, <sup>2</sup>Photon Sciences, Deutsches Elektronen Synchrotron, D-22607 Hamburg, Germany, <sup>3</sup>European XFEL GmbH, D-22869 Schenefeld, Germany, <sup>4</sup>High Pressure Collaborative Access Team (HPCAT), X-ray Science Division, Argonne National Laboratory, Illinois 60439, USA, <sup>5</sup>National Synchrotron Light Source II, Brookhaven National Laboratory, Upton, NY 11973, USA

**Introduction:** High-pressure mineral phases are known to nucleate during and after large meteor impacts [1, 2]. These phases are used to constrain the pressure and temperature conditions reached during impacts [3, 4], which can, in turn, be used to estimate properties of the impactor [2, 5-8]. However, the effects of kinetics and strain-rate on the formation and preservation of these high-pressure phases are relatively unconstrained [5]. Consequently, some mineral assemblages indicate conflicting peak pressures [9], multiple dynamic events [10-11], and/or suggest that both compression and decompression stages of impact may be recorded [12]. In this work, we focus on albite, the Na-end member of the plagioclase feldspar series. With increasing shock pressures and temperatures, albite initially deforms, forms maskelynite and other high-pressure polymorphs, e.g. lingunite, and eventually melts. Dissociation reactions forming jadeite ( $\text{NaAlSi}_2\text{O}_6$ ) and calcium-ferrite type  $\text{NaAlSi}_2\text{O}_4$  have been previously observed [13]. We use simultaneous rapid decompression and laser-heating in the Diamond Anvil Cell (DAC) combined with *in situ* X-ray diffraction to study strain-rate and kinetic effects in albite nucleation and growth.

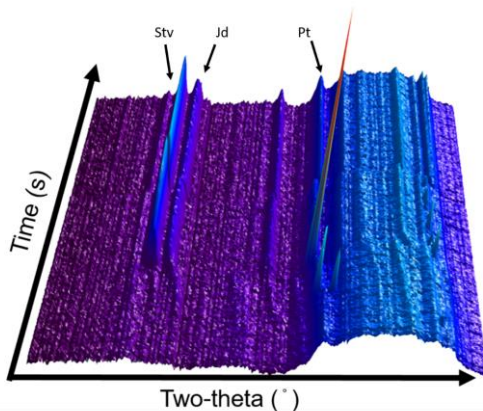


Figure 1. A waterfall plot of diffraction patterns from a typical laser heated decompression experiment on albite. The experimental run starts with an amorphous albite sample and nucleates jadeite and stishovite..

**Experimental Techniques:** We completed a series of laser-heated rapid compression and decompression experiments on natural albite ( $\text{NaAlSi}_3\text{O}_8$ ) from Amelia

County, Va (Sigma-Aldrich) in order to study phase formations and their kinetics. The samples were compressed at room temperature to 30-50 GPa followed by decompression at rates between 0.08(1)-0.90(1) GPa/s. We began laser-heating to temperatures between 1100-1700 K simultaneously with the decompression. X-ray diffraction images were captured every 1 second to determine phase behavior (Fig. 1).

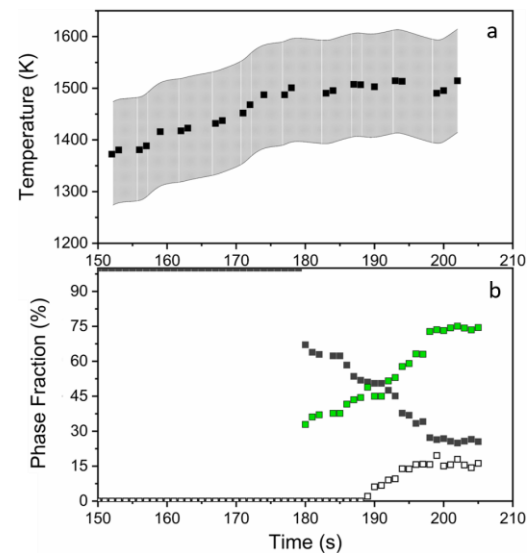


Figure 2. a. Temperature and b. phase fractionation plotted at the time they occur for an experimental run decompressed at 0.27(1) GPa/s. Errors on phase fractions are calculated to be smaller than the data points. White squares are stishovite, green squares are jadeite, black squares are platinum. Platinum appears to decrease with increasing time because it becomes a smaller percentage of the crystalline material.

Rietveld analysis was performed on the integrated X-ray diffraction data to determine the phase fraction of each crystalline phase (Fig. 2). Activation energies were calculated by fitting the curve of the growth behavior of jadeite based on methods from Lin et al., 2017 [14]. The calculated activation energies provide a basis for comparison of behavior with rate. Video of a typical experiment is available on request.

**Results:** During albite fast decompression experiments, jadeite and a  $\text{SiO}_2$  (coesite or stishovite) phase formed. Other high-pressure phases commonly observed in the pressure and temperature range achieved here are markedly absent. The pressure at

which jadeite appeared was lower than the equilibrium nucleation pressure for all runs. The nucleation behavior through time was derived from the diffraction data. The jadeite and SiO<sub>2</sub> phase ratio did not reach stoichiometric equilibrium for any run.

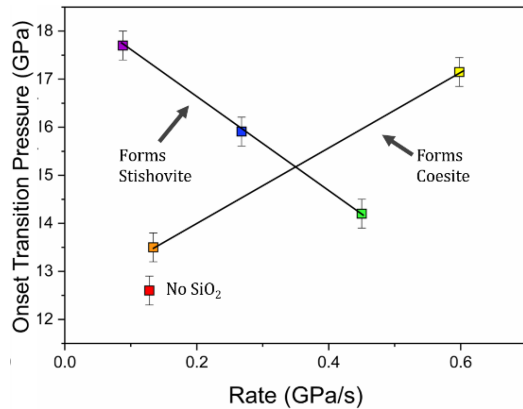


Figure 3. Jadeite nucleation onset pressure plotted vs. decompression rate. Data points correspond to individual runs and are color coded by temperature. Red colors are lowest temperature and blue are highest.

We observed that jadeite can form without a crystalline SiO<sub>2</sub> phase as a result of low temperatures. We also observed intermediate phases that would have produced little evidence of their occurrence if only the recovered sample was examined. We find temperature and decompression rate effects on the onset of nucleation of plagioclase phases (Fig. 3). The activation energy required for jadeite growth increases with increasing decompression rate (Table 1).

Decompression Rate (GPa/s)	SiO <sub>2</sub> Phase	Activation Energy (kJ/mol)	Error (+/-)
0.13	No SiO <sub>2</sub>	0.026	0.0011
0.13	Coe	1.33E-04	4.46E-06
0.6	Coe	0.0074	0.015
0.09	Stv	5.80E-04	2.59E-04
0.27	Stv	0.0014	3.38E-04
0.45	Stv	2.23	0.91

Table 1. Activation energies calculated for jadeite formation for each decompression run. The decompression experiments are organized by which SiO<sub>2</sub> phase is formed during the run. Coe is coesite and Stv is stishovite.

**Discussion:** These experiments have provided us insight into some of the complex interactions that likely take place during natural events and are previously unexplored. Intermediate phases might occur that can alter nucleation paths and therefore imply different formation conditions. Low temperatures can prevent the formation of a crystalline SiO<sub>2</sub> phase, therefore other phases in the mineral assemblage should be examined to rule out this possibility.

**References:** [1] Binns R.A., Davis R.J., and Reed S.J.B. (1969) *Nature*, 221, 943. [2] Chen M. et al. (1996) *Science*, 271, 5255, 1570-1573. [3] Stöffler D., Keil K., and Scott E.R.D. (1991) *Geochim. Cosmochim. Acta*, 55, 12, 3845-3867. [4] Melosh J. (1989) Oxford Uni. Press., 109-111. [5] Sharp T.G. and DeCarli. P. (2006) Uni. of Ariz. Press., 653-677. [6] Gillet P., et al. (2007) *Geol. Soc. Amer.* [7] Gillet P. and El Goresy A. (2013) *Annu Rev Earth Planet Sci.*, 41, 257-285. [8] Langenhorst F. (1994) *Earth Planet. Sci. Lett.*, 128, 3-4, 683-698. [9] Letoulliec R., Pinceaux J.P., and Loubeyre P. (1988) *High Pres. Res.*, 1, 1, 77-90. [10] Miyahara M.E. (2011) *Earth Planet. Sci. Lett.*, 307, 3-4, 361-368. [11] Treiman A. H. (1998) *Meteorit. Planet. Sci.*, 33, 4, 753-764. [12] Walton E.L. et al., (2014) *Geochim. Cosmochim. Acta*, 140, 334-348. [13] Kubo T., M. (2010) *Nat. Geo.*, 3, 1, 41-45. [14] Lin C. et al. (2016) *J. Appl. Phys.*, 119, 4, 045902.

**Acknowledgments:** This work was supported by the National Science Foundation through grant EAR-1440095 and GEO-1107155. LE acknowledges support from NASA through the Solar System Workings program under grant 80NSSC17K0765. TG acknowledges support from the Remote, In Situ and, and Synchrotron Studies for Science and Exploration (RIS4E) node of NASA's Solar System Exploration Research Virtual Institute (SSERVI), NASA Ames Research Center, Moffett Field, CA The high-pressure diffraction experiments were conducted at the Extreme Conditions Beamline (P02.2) at PETRA III at DESY. Portions of this work were performed at HPCAT (Sector 16), Advanced Photon Source (APS), Argonne National Laboratory. HPCAT operations are supported by DOE-NNSA's Office of Experimental Sciences. The Advanced Photon Source is a U.S. Department of Energy (DOE) Office of Science User Facility operated for the DOE Office of Science by Argonne National Laboratory under Contract No. DE-AC02-06CH11357.